The Hybrid Power Flow Controller A New Concept for Flexible AC Transmission

Jovan Z. Bebic
Electric Power and Propulsion Systems Lab
GE Global Research
Niskayuna, NY, USA
Email: bebic@research.ge.com

Peter W. Lehn and M. R. Iravani
Department of Electrical and Computer Engineering
University of Toronto
Toronto, ON, Canada
Email: lehn@ecf.utoronto.ca
Email: iravani@ecf.utoronto.ca

Abstract— **Two novel power flow controller topologies are proposed for flexible AC transmission systems (FACTS). The first one consists of a shunt connected source of reactive power, and two series connected voltage–sourced converters – one on each side of the shunt device. The second topology is a dual of the first; it is based on two shunt connected current–sourced converters around a series connected reactive element. In both cases the converters can exchange active power through a common DC circuit. Both topologies make combined use of passive components and converters and can therefore be regarded as hybrid. Employing hybrid topologies enables use of converters to enhance the functionality of existing equipment in a power system. The paper demonstrates that, by using appropriate converter additions and control, the functionality of switched shunt or series capacitors can be enhanced to generalized power flow control – a functionality commonly associated with the UPFC. Since existing equipment is fully utilized, the hybrid topology requires considerably lower total converter ratings compared to the UPFC.**

I. Introduction

A fundamental characteristic of the power industry is that demand for power rises steadily, while system upgrades are implemented through large and costly projects. Over the years, environmental, right–of–way, and cost problems have delayed construction of both generation facilities and new transmission lines, so better utilization of existing power systems has become imperative. In the early 1980s, it was recognized that a change was needed in the traditional practices used in system planning and operation [1].

Concurrently, technological advancements in the semiconductor industry led to the production of a power grade gate turn–off thyristor (GTO). The commercial availability of GTOs in the mid–1980s made it possible to construct large voltage–sourced converters (VSCs) [2]. In principle, VSCs are capable of generating multiphase alternating voltage of controlled magnitude and phase.

The application of VSCs in the transmission industry became the subject of considerable research effort in the late 1980s and through the 1990s. The "flexible AC transmission system" (FACTS) refers to a concept of power flow control through AC transmission lines using static converters [3]. Examples of converter based FACTS controllers include the advanced static compensator (STATCOM), the series static synchronous compensator (SSSC), the unified power flow controller (UPFC), and the interline power flow controller (IPFC). A comprehensive review of all compensators, classical and modern, can be found in [4].

In the past ten years, pilot installations of STATCOM, UPFC, and IPFC have been built and commissioned [5]–[9]. However, the considerable price of all current FACTS controllers remains as the major impediment to their widespread use. The equipment appropriation for converter based FACTS controllers is further setback by the existence of "classical equipment" – switched capacitors and static VAr compensators (SVCs) for voltage support, and switched series capacitors and thyristor controlled series capacitors (TCSCs) for line impedance control. In many applications these compensators were installed to mitigate critical contingency conditions, and while improvements in their performance would be worth considering, their complete replacement is prohibitive.

It is therefore worthwhile to seek novel and cost effective converter based FACTS topologies that build upon existing equipment and provide improved control performance.

In this paper, two such topologies are presented. The first one consists of a shunt connected controllable source of reactive power, and two series connected voltage–sourced converters – one on each side of the shunt device. The second topology is a dual of the first; it is based on two shunt connected current–sourced converters around a series connected reactive compensator. In both cases the converters can exchange active power through a common DC circuit. Since both topologies make use of converters in addition to the (presumably existing) passive components, they can be regarded as hybrid, and the resulting FACTS controllers are thus named "Hybrid Power Flow Controllers", or HPFC. The analysis carried out in [10] shows that the HPFC offers performance characteristics similar to those of the UPFC. This paper presents some of the results.

The rest of this paper is organized as follows. The HPFC topology that employs series VSCs is introduced in section II. The steady state analysis is given in section III and operating characteristics are derived. The dual topology, based on shunt connected current–sourced converters is presented in section V. Finally, conclusions are given in section VI.

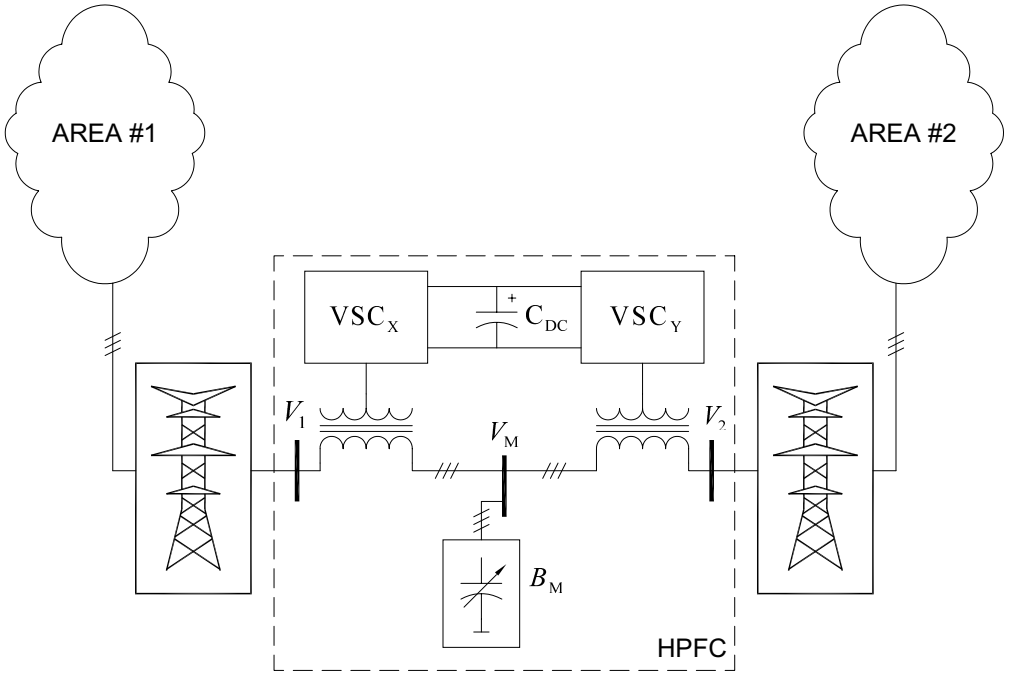

Fig. 1. Hybrid Power Flow Controller – Typical application

II. Proposed Topology

A block diagrammatic view of the envisioned typical HPFC application is shown in Fig. 1. The HPFC is installed on a transmission line that connects two electrical areas. In general, its point of installation will be "within" the transmission line, i.e., at some distance from strong voltage busses.

Central to the HPFC's topology is the shunt connected source of reactive power denoted as B_{M} in Fig. 1 – this can be a switched capacitor bank, or a static VAr compensator. Next, there are two voltage–sourced converters ($\mathrm{VSC_X}$ and $\mathrm{VSC_Y}$) connected in series with the associated line segments using coupling transformers. The converters share a common DC circuit, coupling each other's DC terminals. The DC circuit permits exchange of active power between the converters.

By controlling the magnitudes and angles of voltages supplied by the converters, the flow of active power through the line and the amounts of reactive power supplied to each line segment can be simultaneously and independently controlled. The control of the shunt connected reactive element is coordinated with the control of converters to supply the bulk of the total required reactive power.

A basic comparison of this topology with that of the UPFC highlights the important features of this new circuit. In short, UPFC's shunt converter is substituted by a (presumably existing) switched capacitor, while its series converter is split into two "half-sized" ones, installed on each side of the shunt device. Such topological arrangement results in operating characteristics similar to those of the UPFC, while achieving considerable savings in the total required converter MVA ratings.

III. Steady State Operation

A. Equivalent Circuit

A simplified single–phase equivalent of the circuit of Fig. 1, is shown in Fig. 2. Electrical areas 1 and 2 are represented by their line to neutral Thévenin equivalent voltage sources V_{S} and V_{R}, respectively. The value of parameter $\mathrm{X_S}$ is dominated by the equivalent reactance of the line segment between area 1 and the HPFC, but it includes the Thévenin reactance of area 1, and the leakage reactance of the corresponding converter's coupling transformer. Reactance $\mathrm{X_R}$ has analogous meaning. Losses are neglected for clarity. Indexes "S" and "R" are used to identify "sending" and "receiving" ends of the line.

Voltages V_1, V_2, and V_{M} correspond to the line to neutral voltages at busses labelled in Fig. 1. Voltage sources V_{X} and V_{Y} represent the high voltage equivalents of voltages generated by the $\mathrm{VSC_X}$ and $\mathrm{VSC_Y}$, respectively. The variable capacitance labelled B_{M} represents the switched capacitor. The range of values B_{M} can assume depends on the installed power components; in the general case it can either be positive (capacitive), zero, or negative (inductive).

Active and reactive powers of converters, and areas 1 and 2 are respectively labelled P_{X}, Q_{X}; P_{Y}, Q_{Y}; P_{S}, Q_{S}; and P_{R}, Q_{R}, in Fig. 2. The polarities defined in Fig. 2 will be used in the mathematical description of the system.

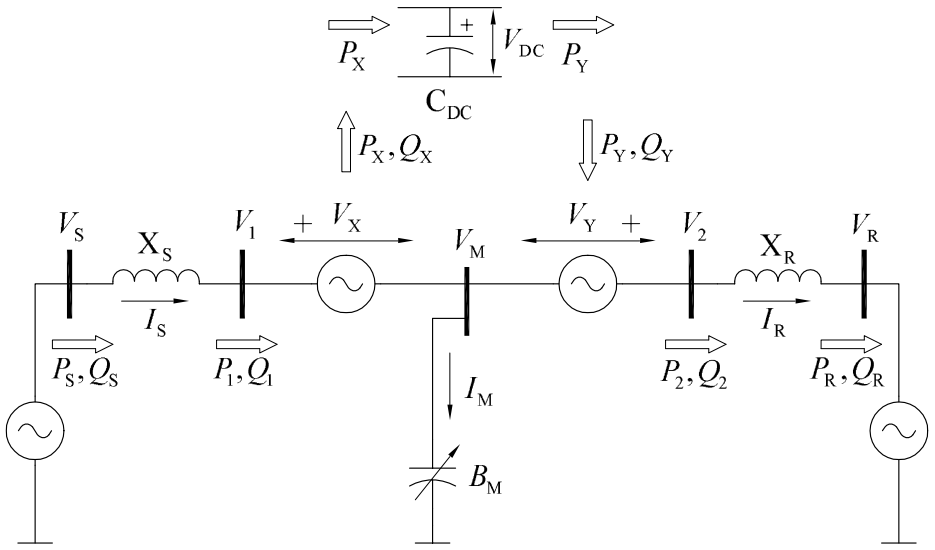

Fig. 2. Hybrid Power Flow Controller – Single phase equivalent circuit

B. Circuit Equations

In order to generalize the formulation with respect to the point of equipment installation, let $\mathrm{X_L}$ and k be defined as:

$$\mathrm{X_L} = \mathrm{X_S} + \mathrm{X_R} \tag{1}$$

$$\mathrm{k} = \frac{\mathrm{X_S}}{\mathrm{X_L}} \tag{2}$$

$\mathrm{X_L}$ thus represents the total line reactance, while k quantifies the "electrical distance" of the HPFC from the sending end.

Next, let the following phasors be introduced:

$$\vec{\mathbf{V}}_\mathrm{S} = V_\mathrm{S}\angle\delta_\mathrm{S} \tag{3}$$

$$\vec{\mathbf{V}}_\mathrm{R} = V_\mathrm{R}\angle\delta_\mathrm{R} \tag{4}$$

$$\vec{\mathbf{V}}_\mathrm{X} = V_\mathrm{X}\angle\delta_\mathrm{X} \tag{5}$$

$$\vec{\mathbf{V}}_\mathrm{Y} = V_\mathrm{Y}\angle\delta_\mathrm{Y} \tag{6}$$

The steady–state (phasor) equations of the AC portion of the circuit are:

$$\begin{aligned} j\mathrm{k}\mathrm{X_L}\vec{\mathbf{I}}_\mathrm{S} + \frac{1}{jB_\mathrm{M}}(\vec{\mathbf{I}}_\mathrm{S} - \vec{\mathbf{I}}_\mathrm{R}) &= \vec{\mathbf{V}}_\mathrm{S} - \vec{\mathbf{V}}_\mathrm{X} \\ -\frac{1}{jB_\mathrm{M}}(\vec{\mathbf{I}}_\mathrm{S} - \vec{\mathbf{I}}_\mathrm{R}) + j(1-\mathrm{k})\mathrm{X_L}\vec{\mathbf{I}}_\mathrm{R} &= -\vec{\mathbf{V}}_\mathrm{R} + \vec{\mathbf{V}}_\mathrm{Y} \end{aligned} \tag{7}$$

The common DC circuit permits exchange of active power between the converters. With polarities shown in Fig. 2, positive P_X results in the positive charging current for $\mathrm{C_{DC}}$, while positive P_Y results in the negative charging current. In order to maintain a fixed charge on $\mathrm{C_{DC}}$, the converters have to operate under the "constraint of power balance", i.e.,

$$\mathrm{Re}\left\{\vec{\mathbf{V}}_\mathrm{X}\vec{\mathbf{I}}_\mathrm{S}^*\right\} = \mathrm{Re}\left\{\vec{\mathbf{V}}_\mathrm{Y}\vec{\mathbf{I}}_\mathrm{R}^*\right\} \tag{8}$$

C. Finding Viable Steady–State Operating Points

A "viable" steady–state operating point can now be defined as a solution for circuit voltages and currents that simultaneously satisfy the circuit equations (7), and the constraint of power balance (8).

In [11], the authors proposed a geometric method for solving the viable operating points of the UPFC. The key feature of the proposed methodology is that it considers the power balance of the converters indirectly, at the system level rather than the equipment level.

The same principle can be used here. Namely, for any steady–state operating point, the energy stored in the HPFC and in the line reactances is constant; hence, in a lossless system, all power supplied to the circuit at the sending end is delivered to the receiving end. Consequently, the power balance expressed by (8) can be replaced by:

$$P_\mathrm{S} = P_\mathrm{R}; \tag{9}$$

that is:

$$\mathrm{Re}\left\{\vec{\mathbf{V}}_\mathrm{S}\vec{\mathbf{I}}_\mathrm{S}^*\right\} = \mathrm{Re}\left\{\vec{\mathbf{V}}_\mathrm{R}\vec{\mathbf{I}}_\mathrm{R}^*\right\} \tag{10}$$

Consider now the geometric interpretation of (10). Specifying $P_\mathrm{S} = P_\mathrm{ref}$ is equivalent to stipulating that $\vec{\mathbf{I}}_\mathrm{S}$ must have its tip on a specific line perpendicular to $\vec{\mathbf{V}}_\mathrm{S}$, as shown in Fig. 3(a). Analogously, stipulating that $P_\mathrm{R} = \mathrm{const}$ prescribes that the tip of $\vec{\mathbf{I}}_\mathrm{R}$ lie on a line perpendicular to $\vec{\mathbf{V}}_\mathrm{R}$. Let this pair of lines be named the "pair of equal power lines" or "equal power lines" for short.

It follows that maintaining power balance between the converters can be interpreted as the requirement to maintain the tips of $\vec{\mathbf{I}}_\mathrm{S}$ and $\vec{\mathbf{I}}_\mathrm{R}$ on a pair of equal power lines.

It is now possible to describe a procedure for solving the viable operating points directly, based on the specified P_ref, Q_Sref, and Q_Rref. Fig. 3(a)–(c) graphically demonstrate the exemplary steps.

First, for a given value P_ref, and known $\vec{\mathbf{V}}_\mathrm{S}$ and $\vec{\mathbf{V}}_\mathrm{R}$, a pair of equal power lines is drawn as shown in Fig. 3(a).

Next, $\vec{\mathbf{I}}_\mathrm{S}$ and $\vec{\mathbf{I}}_\mathrm{R}$ are chosen to select the desired Q_Sref and Q_Rref, respectively. With $\vec{\mathbf{I}}_\mathrm{S}$ and $\vec{\mathbf{I}}_\mathrm{R}$ known, $\vec{\mathbf{I}}_\mathrm{M}$, $\vec{\mathbf{V}}_1$, and $\vec{\mathbf{V}}_2$

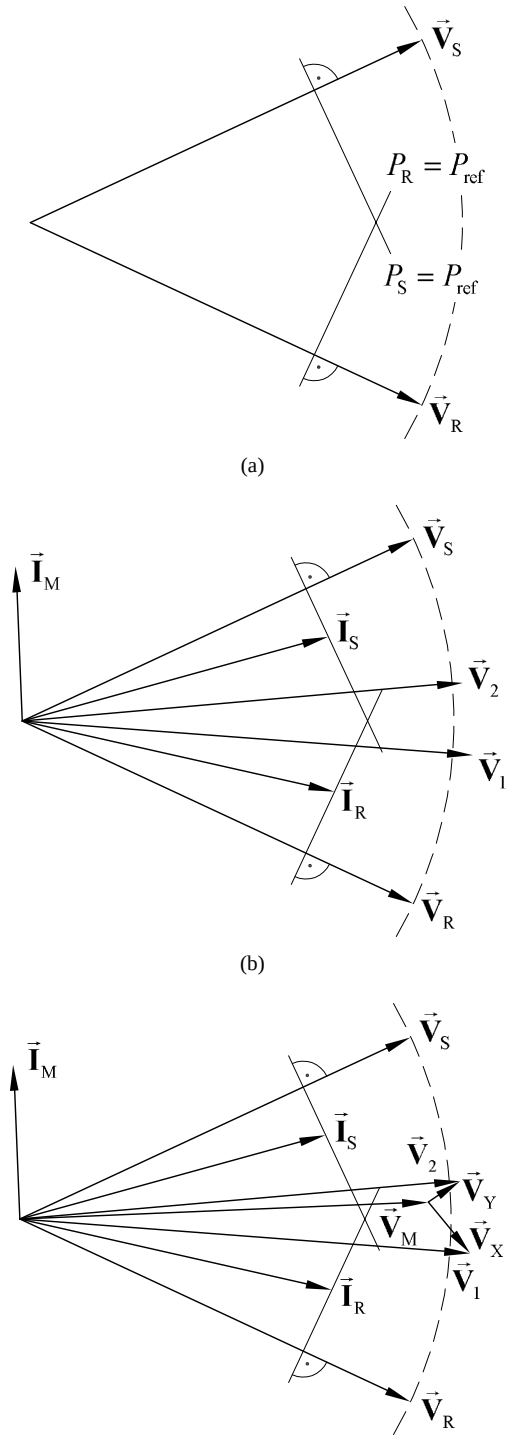

Fig. 3. Example procedure for solving steady state operating points based on specified $P_{\rm ref}$, $Q_{\rm Sref}$, and $Q_{\rm Rref}$

are readily obtained from:

$$\vec{\mathbf{I}}_{\rm M} = \vec{\mathbf{I}}_{\rm S} - \vec{\mathbf{I}}_{\rm R} \quad (11)$$

$$\vec{\mathbf{V}}_1 = \vec{\mathbf{V}}_{\rm S} - j{\rm k}{\rm X}_{\rm L}\vec{\mathbf{I}}_{\rm S} \quad (12)$$

$$\vec{\mathbf{V}}_2 = \vec{\mathbf{V}}_{\rm R} + j(1-{\rm k}){\rm X}_{\rm L}\vec{\mathbf{I}}_{\rm R}. \quad (13)$$

An example choice of $\vec{\mathbf{I}}_{\rm S}$ and $\vec{\mathbf{I}}_{\rm R}$ (matching the user specified $P_{\rm ref}$, $Q_{\rm Sref}$, and $Q_{\rm Rref}$) and the resulting $\vec{\mathbf{I}}_{\rm M}$, $\vec{\mathbf{V}}_1$, and $\vec{\mathbf{V}}_2$ (according to (11)–(13)) are shown in Fig. 3(b).

Finally, $\vec{\mathbf{V}}_{\rm M}$, $\vec{\mathbf{V}}_{\rm X}$, and $\vec{\mathbf{V}}_{\rm Y}$ are found from:

$$\vec{\mathbf{V}}_{\rm M} = \frac{-j}{B_{\rm M}}\vec{\mathbf{I}}_{\rm M} \quad (14)$$

$$\vec{\mathbf{V}}_{\rm X} = \vec{\mathbf{V}}_1 - \vec{\mathbf{V}}_{\rm M} \quad (15)$$

$$\vec{\mathbf{V}}_{\rm Y} = \vec{\mathbf{V}}_2 - \vec{\mathbf{V}}_{\rm M}. \quad (16)$$

The resulting complete phasor diagram is shown in Fig. 3(c).

IV. Functional Capabilities of the HPFC

The procedure explained in section III-C, can be used to solve ample number of viable operating points and explore the functional capabilities of the HPFC. Several illustrative phasor diagrams are presented in this section.

Consider first the diagram in Fig. 4(a) – it represents the "natural" power flow between two directly interconnected areas. The natural power flow between $\vec{\mathbf{V}}_{\rm S}$ and $\vec{\mathbf{V}}_{\rm R}$ is given by the well–known formula [12]:

$$\vec{\mathbf{P}}_0 = 3\frac{|\vec{\mathbf{V}}_{\rm S}||\vec{\mathbf{V}}_{\rm R}|}{{\rm X}_{\rm L}}\sin(\delta) \quad (17)$$

where δ represents the angle between $\vec{\mathbf{V}}_{\rm S}$ and $\vec{\mathbf{V}}_{\rm R}$, i.e., $\delta = \delta_{\rm S} - \delta_{\rm R}$.

The HPFC can change this power flow. In the case of the operating point shown in Fig. 4(b), reduction of power flow is achieved by injecting voltages $\vec{\mathbf{V}}_{\rm X}$ and $\vec{\mathbf{V}}_{\rm Y}$ so as to reduce the angular differences between $\vec{\mathbf{V}}_{\rm S}$ and $\vec{\mathbf{V}}_1$, and $\vec{\mathbf{V}}_2$ and $\vec{\mathbf{V}}_{\rm R}$, respectively.

The diagram in Fig. 4(c) is constructed using the same values for line currents, but a different value for $B_{\rm M}$. The resulting $\vec{\mathbf{V}}_{\rm M}$ is hence of larger magnitude and the corresponding $\vec{\mathbf{V}}_{\rm X}$ and $\vec{\mathbf{V}}_{\rm Y}$ are different. The comparison of Figs. 4(b) and (c) illustrates that step–changed value of the shunt susceptance can be used to lower the voltage ratings of the converters ${\rm VSC}_{\rm X}$ and ${\rm VSC}_{\rm Y}$. Thus, passive $B_{\rm M}$ is used to effectively replace the converter ratings.

The HPFC has the ability to independently control the amount of reactive power exchanged with the sending and receiving ends of the line. This is demonstrated in Fig. 4(d) where Q_2 has been increased ($Q_{\rm Rref}$ reduced), resulting in new $\vec{\mathbf{V}}_{\rm M}$, $\vec{\mathbf{V}}_{\rm X}$, and $\vec{\mathbf{V}}_{\rm Y}$. The locations of vectors corresponding to the operating point of Fig. 4(b) are shown in dashed lines to help quantify the difference.

A phasor diagram corresponding to increased power flow is shown in Fig. 4(e). Increase in magnitudes of $\vec{\mathbf{I}}_{\rm S}$ and $\vec{\mathbf{I}}_{\rm R}$ is a result of increased relative angles between $\vec{\mathbf{V}}_{\rm S}$ and $\vec{\mathbf{V}}_1$, and $\vec{\mathbf{V}}_2$ and $\vec{\mathbf{V}}_{\rm R}$, respectively. In this case $\vec{\mathbf{V}}_2$ will lead $\vec{\mathbf{V}}_1$.

The above discussion demonstrates that, from the perspective of steady state operation, the HPFC can be regarded as the functional equivalent of the UPFC.

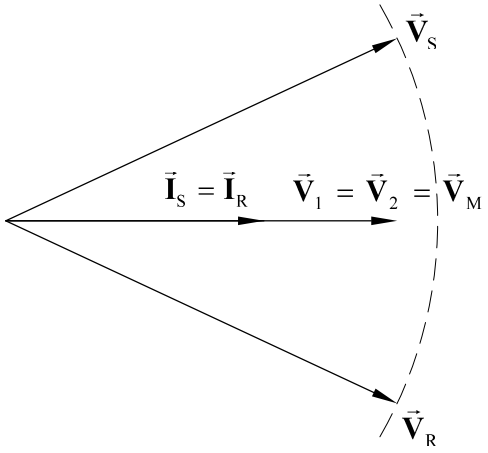

(a) Natural power flow $\vec{\mathbf{V}}_X = \vec{\mathbf{V}}_Y = 0$, $B_M = 0$

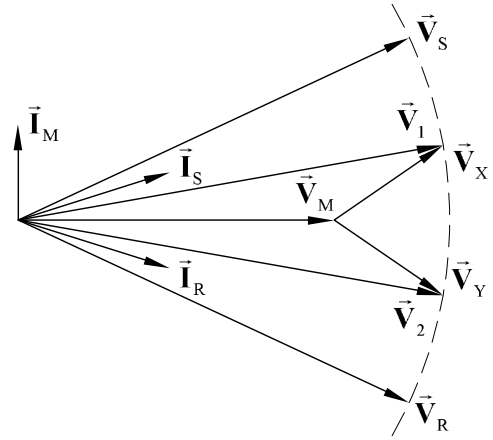

(b) Reduced power flow

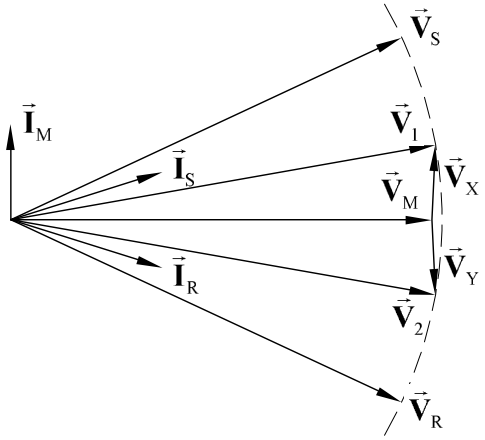

(c) B_M control reduces converter voltages

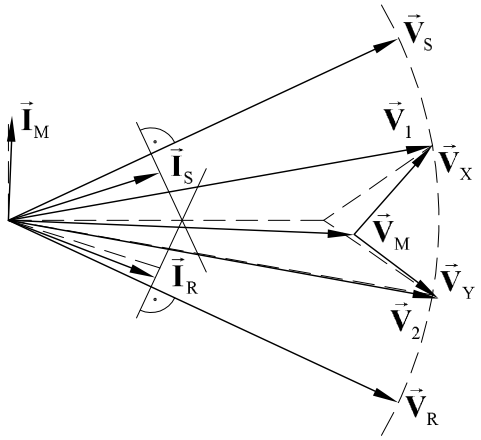

(d) Decoupled control of Q_2

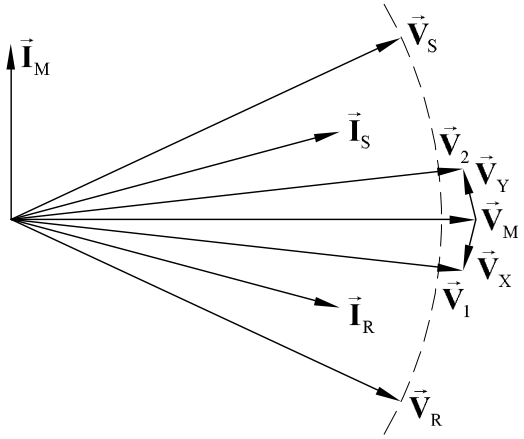

(e) Increased power flow

Fig. 4. Hybrid Power Flow Controller – Example phasor diagrams

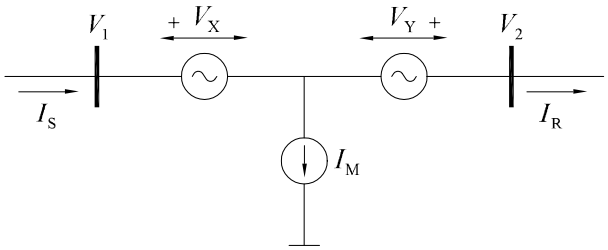

(a) Equivalent of the original circuit

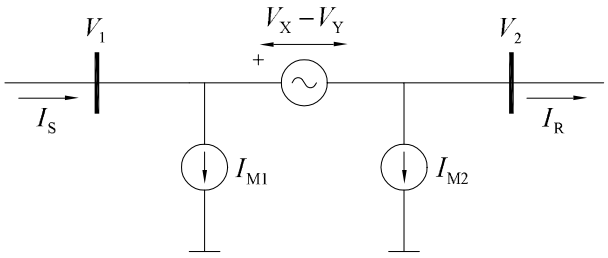

(b) Rearranged equivalent sources

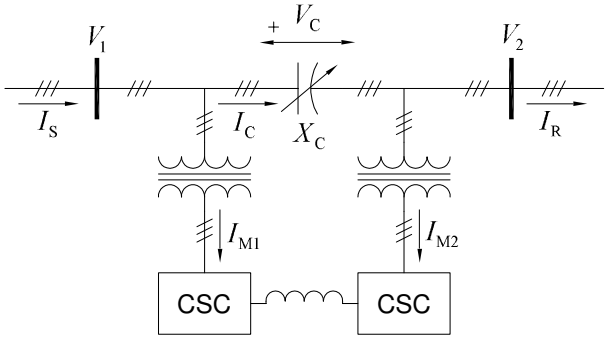

(c) Final circuit employing a series connected reactance

Fig. 5. Hybrid Power Flow Controller – Circuit transformations

V. Dual Topology

A valuable dual topology to the circuit of Fig. 2 can be obtained by following the simple circuit transformations shown in Fig. 5. As a starting point, let the shunt connected variable susceptance be replaced by the shunt connected current source, as shown in Fig 5(a). Next, let this current source be split into two "half sized" ones and the two voltage sources combined into one, as shown in Fig 5(b). Finally, let the series connected voltage source be regarded as a variable reactance, and the shunt connected current sources as current–sourced converters and a dual HPFC topology is obtained – Fig. 5(c).

As in the case of the original circuit, the converters couple each other's DC terminals, and hence are able to exchange active power. This topological variant of the HPFC can be used to improve the performance of series capacitors.

Viable operating points can be obtained by following a procedure analogous to the one explained in section III-C; as before, $\vec{\mathbf{I}}_{\mathrm{S}}$ and $\vec{\mathbf{I}}_{\mathrm{R}}$ are selected based on the specified P_{ref}, Q_{Sref}, and Q_{Rref}. $\vec{\mathbf{V}}_1$, and $\vec{\mathbf{V}}_2$ are then obtained using (12)

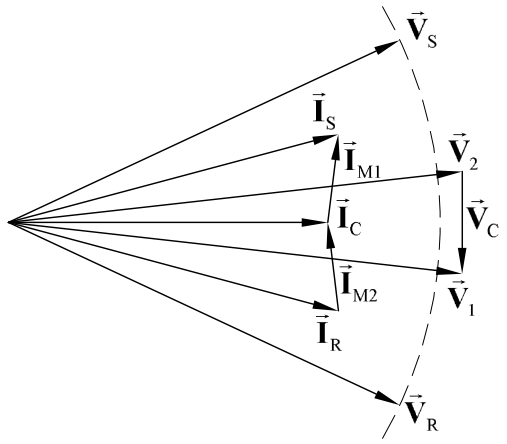

Fig. 6. Hybrid Power Flow Controller – Dual circuit's phasor diagram

and (13), respectively. Next, $\vec{\mathbf{V}}_{\mathrm{C}}$ and $\vec{\mathbf{I}}_{\mathrm{C}}$ are found from:

$$\vec{\mathbf{V}}_{\mathrm{C}} = \vec{\mathbf{V}}_1 - \vec{\mathbf{V}}_2 \quad (18)$$

$$\vec{\mathbf{I}}_{\mathrm{C}} = \frac{-j}{X_{\mathrm{C}}}\vec{\mathbf{V}}_{\mathrm{C}} \quad (19)$$

where X_{C} is the value of engaged series reactance; $X_{\mathrm{C}} = -1/\omega C$ when X_{C} is dominantly capacitive, or $X_{\mathrm{C}} = \omega L$ when X_{C} is dominantly inductive. Finally, $\vec{\mathbf{I}}_{\mathrm{M1}}$ and $\vec{\mathbf{I}}_{\mathrm{M2}}$ are found from:

$$\vec{\mathbf{I}}_{\mathrm{M1}} = \vec{\mathbf{I}}_{\mathrm{S}} - \vec{\mathbf{I}}_{\mathrm{C}} \quad (20)$$

$$\vec{\mathbf{I}}_{\mathrm{M2}} = \vec{\mathbf{I}}_{\mathrm{C}} - \vec{\mathbf{I}}_{\mathrm{R}}. \quad (21)$$

The complete phasor diagram is shown in Fig. 6.

VI. Conclusions

Two promising power flow controller topologies have been introduced. The first one utilizes a shunt connected source of reactive power and uses two series connected voltage–sourced converters to achieve direct line control. The second topology is the dual of the first; it is based on two shunt connected current–sourced converters around a series connected reactive compensator. Both topologies make combined use of passive components and converters, and can therefore be regarded as hybrid.

A methodology for solving viable operating points of the HPFC has been proposed. The methodology is based on the equal power lines concepts introduced in [11]. The applicability of the equal power lines concept to both topological variants of the HPFC, in addition to the UPFC, demonstrates its universal value.

The functional capabilities of the HPFC were discussed using representative phasor diagrams. It was shown that the HPFC can be used to simultaneously and independently control the flow of active power through the line and the amounts of reactive power exchanged with the sending and receiving end. Thus, the performance characteristics of the HPFC were shown to be similar to those commonly associated with the UPFC.

The ability of the HPFC to fully utilize the hardware of classical compensators – switched shunt capacitors, SVCs, series capacitors, and TCSCs – is expected to ensure a promising commercial future for this new concept.

REFERENCES

[1] N. Hingorani, "Power Electronics in Electric Utilities: Role of Power Electronics in Future Power Systems," *Proceedings of the IEEE*, vol. 76, no. 4, pp. 481–482, Apr. 1988.

[2] L. Gyugyi, "Dynamic Compensation of AC Transmission Lines by Solid-State Synchronous Voltage Sources," *IEEE Trans. Power Delivery*, vol. 9, no. 2, pp. 904–911, Apr. 1994.

[3] N. Hingorani, "High Power Electronics and Flexible AC Transmission System," *IEEE Power Engineering Review*, vol. 8, no. 7, pp. 3–4, July 1988.

[4] N. G. Hingorani and L. Gyugyi, *Understanding FACTS, Concepts and Technology of Flexible AC Transmission System*. IEEE Press, 2000.

[5] C. Schauder, M. Gernhardt, E. Stacey, T. Lemak, L. Gyugyi, T. Cease, and A. Edris, "Development of a 100 MVAr Static Condenser for Voltage Control of Transmission Systems," *IEEE Trans. Power Delivery*, vol. 10, no. 3, pp. 1486–1496, July 1995.

[6] ——, "Operation of 100 MVAr TVA STATCON," *IEEE Trans. Power Delivery*, vol. 12, no. 4, pp. 1805–1811, Oct. 1997.

[7] M. Rahman, M. Ahmed, R. Gutman, R. O'Keefe, R. Nelson, and J. Bian, "UPFC Application on the AEP System: Planning Considerations," *IEEE Trans. Power Systems*, vol. 12, no. 4, pp. 1695–1701, Nov. 1997.

[8] A. Mehraban, A. Edris, C. Schauder, and J. Provanzana, "Installation, Commissioning, and Operation of the World's First UPFC on the AEP System," in *Proceedings of International Conference on Power System Technology, POWERCON '98*, vol. 1, 1998, pp. 323–327.

[9] S. Zelingher, B. Fardanesh, B. Shperling, S. Dave, L. Kovalsky, C. Schauder, and A. Edris, "Convertible static compensator project-hardware overview," in *Proceedings of Power Engineering Society Winter Meeting*, vol. 4, 2000, pp. 2511–2517.

[10] J. Bebic, "A Symmetrical Hybrid Power Flow Controller," Ph.D. dissertation, Univ. of Toronto, Toronto, Sept. 2003.

[11] J. Z. Bebic, P. W. Lehn, and M. R. Iravani, "P–δ Characteristics for the Unified Power Flow Controller – Analysis Inclusive of Equipment Ratings and Line Limits," *IEEE Trans. Power Delivery*, vol. 18, no. 3, pp. 1066–1072, July 2003.

[12] W. D. Stevenson, *Elements of Power Systems Analysis*. McGraw–Hill, 1989.